

Study of a Direction Sensitive Photo-Sensor

Zach Parsons

Office of Science, SULI Program

University of South Dakota

Brookhaven National Laboratory

Upton, New York

August 9, 2004

Prepared in partial fulfillment of the requirements of the Office of Science, DOE Student Undergraduate Laboratory Internship (SULI) Program under the direction of Dr. Milind Diwan in the Electronic Detector Group (EDG) at Brookhaven National Laboratory.

Participant:

Signature

Research Advisor:

Signature

Table of Contents

Abstract

Introduction

Water Cherenkov Detector

Liquid Scintillator Detector

Requirements

Initial Design

Material Selection

Design

Conclusions

Acknowledgements

References

Figures and Tables

Abstract

Study of a Direction Sensitive Photo-Sensor. ZACH PARSONS (University of South Dakota, Vermillion, SD, 57069) MILIND DIWAN (Brookhaven National Laboratory, Upton, New York, 11973).

A charged particle traveling through a medium will polarize the medium creating radiation. If the speed of the particle is greater than the speed of light in that medium, the radiation is emitted as a coherent wave front known as Cherenkov radiation. The photons all have the same angle with respect to the direction of the particle. This radiation is similar to the sonic boom heard from supersonic aircraft. This Cherenkov radiation can be detected by photo sensors to understand properties of the charged particles. Today's large water Cherenkov detectors, like Super Kamiokande in Japan, use photomultiplier tubes (PMT's) to detect the photons. In this report, we studied a new kind of photo detector, a direction sensitive PMT, which uses a lens to transfer the incident photon angle to a position on a detecting surface. We have studied a basic wide angle lens design. The lens was altered to make it cost effective, while at the same time efficient. The resolution of the lens was relaxed in exchange for the tightening of several other parameters. The parameters that were studied included lens thickness, image plane area, system aperture, and distance from lens to image plane.

Introduction

In this paper we have studied the optical configuration of a direction sensitive photo-sensor (DSPS). In many applications in particle and nuclear physics experiments, it could be advantageous to measure the propagation direction of individual scintillation or Cherenkov photons. Such a measurement is possible by using appropriate mirrors or lenses in combination with position sensitive photon detectors. An example of such a detector was described by Thomas Ypsilantis in [1].

To first order a simple lens or a mirror acts as an angle to position converter. Photons that are incident at the same angle anywhere in the lens aperture are focused to the same point on the focal surface. By measuring the position on the focal surface we can measure the incoming direction of the light. In a large particle physics detector (for example, the Super-Kamiokande detector in Japan [2]) photons are detected by photo-multiplier tubes. If these tubes were to be replaced by direction sensitive photo-sensors then we could obtain the direction of each detected photon. Knowledge of the location of the DSPS and the photon direction with good resolution will greatly aid the reconstruction of events. It should also improve particle identification, energy resolution, and reconstruction of events with multiple particles.

In the following, we first briefly describe the anticipated applications to either water Cherenkov or liquid scintillation detectors. We list the requirements for the DSPS. Using these requirements we make an initial design of the optics. Using the computer program ZEMAX [3] we optimize the design and calculate the possible field of view, angular resolution, and absorption of light. Finally we will make remarks on the construction of such a detector.

Water Cherenkov Detector

When a charged particle travels in a medium with an index of refraction (n) with velocity larger than the speed of light in that medium (c/n), a cone of light is emitted. This effect is known as Cherenkov light after the discoverer of this radiation. The half angle θ_c of the Cherenkov cone for a particle with velocity β in a medium with index of refraction n is

$$\theta_c = \arccos(1/n\beta)$$

The Cherenkov light emission in water per unit wavelength and per unit path length of a charged particle is described by the following formula:

$$\frac{d^2 N}{dx d\lambda} = \frac{2\pi\alpha z^2}{\lambda^2} \times \left(1 - \frac{1}{\beta^2 n^2(\lambda)}\right)$$

Here λ is the wavelength of light, x is the path length, β is the velocity of the particle in units of the speed of light, and $n(_)$ is the index of refraction as a function of wavelength. In addition, α and z are the fine structure constant and the charge of the particle in units of e . Typical values for water are $n=1.33$, and $\theta_c = 41.2$ deg for relativistic particles. When we integrate the above equation over the wavelengths 300 to 600 nm, the yield is about 328 photons per cm of track for relativistic particles in water. Absorption of the light in water and the efficiency of the photo-sensor lower the yield.

In figure 1 we show the calculated spectrum of photons in pure water versus wavelength in nm. The spectrum was calculated using full GEANT [4] simulation in which 1 GeV/c muons were simulated at the center of a 50 meter diameter and 50 meter high water tank. The Cherenkov light produced by the muon (as well as associated delta rays) was transported through water accounting for absorption using the measured

absorption lengths [5] to the inner surface of the tank. The upper curve in figure 1 is the spectrum expected at the inner surface of the tank normalized to unit area. The Cherenkov spectrum, as shown in above equation, increases at shorter wavelengths as $1/\lambda^2$. This increase at shorter wavelengths gets sharply cut off because of absorption below 300 nm. There is also strong absorption above 600 nm. Traditional photocathode efficiency peaks around 370 nm. The second curve in Figure 1 shows the spectrum after accounting for the quantum efficiency of a typical bi-alkali photocathode. It is clear that significant improvement is possible if a new photo-sensor can be made more efficient in the 300 to 400 nm (near ultraviolet) region.

One of the most demanding potential applications for the DSPS will be a new very large underground water Cherenkov detector for long baseline neutrino physics [6]. At present, Super Kamiokande (SK) detector in Japan (see Figure 2) is the largest water Cherenkov detector in the world and it has been used to detect neutrinos from the sun as well as the atmosphere [2]. The SK detector has 50 kT of pure water viewed by approximately 11000 photo-multiplier tubes (PMTs), each with a diameter of 50 cm. In such water Cherenkov detectors, high energy charged particles (such as electrons, muons etc.), produced upon neutrino interactions, create the Cherenkov photons (from UV to visible range). These photons are viewed by the photo-multiplier tubes placed on the walls of the tank, and the measurement of time (with few nanosecond resolution) and charge at each PMT can be used to reconstruct the trajectory of the particle.

The next generation detector of this kind is being considered for several different locations and will need to be at least 500kT in mass. The physics agenda for such a large detector includes proton decay [7], detection of neutrinos from astrophysical sources

(such as the sun, cosmic rays, and super-novae), and man made sources such as accelerators. The photo-sensor for such a large detector will be very challenging. It must have good efficiency over the wavelength range shown in Figure 1. It should have good ($< \text{few ns}$) timing response. Since the photo-sensor will be mounted on the wall of the tank, it must have very wide angular acceptance so that light at high angles to the tank's surface, caused by events near the edges of the tank, can be detected. The photo-sensor must have large area and have low cost to be able to cover the large surface area. For a direction sensitive sensor, the angular resolution is an important parameter. For a muon particle of few GeV, multiple scattering limits the angular resolution to 2 deg. It is therefore unnecessary to have resolution better than 2 deg. On the other hand, to obtain the needed improvement in particle tracking and event identification, it will be necessary to have resolution better than about 5 deg.

Liquid Scintillator Detector

Our design for a direction sensitive photo-sensor could be useful for a liquid scintillator based calorimetric detector. In such a detector a large volume of organic liquid scintillator is placed in a tank and viewed by photomultiplier tubes on the inner wall. The largest such detector so far is the KAMLAND detector also at Kamioka [8]. The various materials and mechanism of scintillation are reviewed by the PDG [9].

Typical densities for liquid scintillator are in the range of 0.9 – 1.2 gm/cc. Typical photon yields are about 1 photon per 100 eV of energy deposit. A minimum ionizing particle traversing 1 cm will yield $\sim 2 \times 10^4$ photons depending on the concentration of the fluors in the medium. Typical wavelength of scintillation light is in the blue-green range. The amount of light detected in photomultiplier tubes depends on

the attenuation length of the medium (~ 1 -- 5 meters), the quality of the optical coupling between the scintillator and the photo-detector, and the efficiency of the photo-detector for blue-green light ($\sim 20\%$). Unlike Cherenkov light, scintillation light is emitted isotropically; therefore the pattern of light has little information about the original position or direction of the particle. A direction sensitive photo-sensor will, however, allow the tracking of individual emitted photons. By using enough statistics and tracking photons back to their origin it is possible to reconstruct an image of the particle track. Such a tomographic technique could be important for lowering backgrounds in future large (multi-kilo-ton) experiments to measure neutrino interactions from the sun or reactors.

Requirements

For our design of the DSPS, we focus on the water Cherenkov application. It is very likely that with a few changes the same design could be used for a liquid scintillator detector. For this initial design study we attempt to meet the following requirements:

1. Aperture size of at least 10 cm.
2. Angular acceptance of ± 60 degree or larger.
3. Angular resolution of at least 5 degrees.
4. Sensitivity for photons in the wavelength range from 300 to 500 nm.
5. We will assume that the optical interfaces are water-lens-vacuum.
6. We focus on a design with a single lens and a geometry that will lead to a simple robust package that is relatively simple to construct.

7. Eventually for a real design we will have to design the high voltage and signal feedthroughs as well as the vacuum seals, but for the exercise in this paper we limit ourselves to the design of the optics.

Initial Design

It is clear that the large aperture and the angular acceptance will require the lens to be thick. Most of the power of the lens will come from the interface with vacuum because the difference in indices of refraction at the water-lens interface will be small. Angular resolution will be dominated by spherical aberrations; therefore long focal lengths are preferred. But to keep the photo-sensor area (the focal plane) small the lens will need to have as short a focal length as possible. The large aperture size, small focal length, large angular acceptance with good resolution, and small focal plane area are conflicting requirements. The best way to optimize is to use the ZEMAX software program which allows such optimization by means of the merit function [3].

In this section, we will calculate simple properties of a thick lens which has one interface with water and the other interface with vacuum. We will calculate the properties of this lens in the paraxial approximation which assumes that all angles are small. The results we obtain will be good to only first order, and will not be valid for large angles. But from this exercise we will get insight into the optimization that will yield the type of lens we want.

Our simple exercise is illustrated in Figure 3. We will assume that the lens is made of glass with index of refraction $n_2=1.5$. Index of refraction for water is $n_1=1.33$. We will assume that the thickness of the lens is $d=30$ mm. The radius of curvature for the water-lens interface is $R_1=100$ mm with center at C_1 . The radius of curvature for the

lens-vacuum interface is $R_2=100$ mm with center at C_2 . D_1 and D_2 are called the power of the interface.

$$D_1 = \frac{(n_2 - n_1)}{R_1} \quad D_2 = \frac{(n_2 - n_3)}{R_2}$$

For our geometry we are interested in light coming from water and going to vacuum. We will first consider the case where the light from the water is parallel to the axis of the lens. Using the method of principal planes [10] we calculate the distance of the second principal plane, P_2 , from the lens-vacuum interface to be h_2 .

$$H_2 = \frac{\frac{d \times D_1}{n_2}}{\frac{D_1}{n_3} + \frac{D_2}{n_3} - \frac{d \times D_1 \times D_2}{n_2 \times n_3}}$$

For our present exercise, $h_2 = 5.2$ mm. The point of focus on the vacuum side is at F_2 .

The focal distance between P_2 and F_2 is given by the focal length, f_2 .

$$\frac{1}{f_2} = \frac{(D_1 + D_2)}{n_3} - \frac{d \times D_1 \times D_2}{n_2 \times n_3}$$

For our present exercise, $f_2 = 153$ mm. We now make several observations that will lead us to an optimized lens design.

The majority of the bending power of the lens is coming from the second, lens-vacuum, interface because of the higher difference in indices of refraction. The easiest way to achieve a lens with a large aperture is with a long focal length using only the second interface. If both interfaces have finite radii of curvature, then the size of the lens will be limited as can be seen in Figure 3.

For rays obliquely incident on the lens, the point of focus will not be on a plane located at F_2 . In general, it will be on a spherical surface as shown in Figure 4. We will

allow the focal plane to be a curved surface, so that photons with incident angles up to 60 deg can be focused to a point. As Figure 4 shows the area of the focal surface, which must be covered by expensive photo-sensitive medium, is proportional to the angular coverage required and the square of the focal length. It is therefore important to achieve a short focal length.

The angular resolution on the focal surface will be caused by spherical and chromatic aberrations. As focal length is made short, the lens thickness and curvature will increase and the main contributor to the angular resolution will be spherical aberrations. ZEMAX will allow us to accurately estimate the angular resolution for several different geometries.

In Figure 5, we show two possible geometries for detecting the photons focused by the lens. In the first method (in the upper part of the figure) the entire focal plane is covered by photo-cathode material. The incident photon will cause an electron to be emitted from this surface. A high voltage electric field is shaped in such a way as to accelerate this electron by several thousand volts and transport it to a unique position on a silicon detector. This detector will need to have sufficient position resolution (achieved either by pixels or by charge interpolation) to achieve the needed angular resolution. The second method is illustrated in the bottom of the figure. In this method, we would simply place photo-detectors, either photo-multiplier tubes or avalanche photo-diodes at the focal surface in a large array. The second method will clearly need a very large number of detectors compared to the first one, and the angular resolution will be limited by the size of the photomultipliers. In any case, to construct the device envisioned in Figure 5, much R&D is needed in several areas: creating the needed high vacuum, depositing

photo-cathode on the focal surface, constructing and operating the position sensitive electron detector, and providing high voltage to the photo-cathode. In this paper we intend to solve the problem of the optics only.

Material Selection

As shown in figure 1, the bulk of the Cherenkov radiation is found between 325 and 450 nm. Finding materials to transmit at 400 nm does not pose a challenge; however, as you start to look at ultraviolet wavelengths the transmission of many materials begins to drop off significantly. There are a limited number of optical materials which transmit such low wavelengths efficiently. The other factor in deciding upon a material is its index of refraction. The index needs to be large enough to refract the rays significantly enough, yet not so large that a significant fraction of the light is reflected.

One of the materials selected for this study is polycarbonate. Polycarbonate's index of refraction is 1.586, and its transmission over most of the Cherenkov spectrum is approximately eighty to eighty-five percent. However, at UV wavelengths lower than 350 nm the transmission of polycarbonate begins to drop off dramatically as shown in figure 6 [11]. Transmission is figured using the formula

$$T = e^{-x/x_0}$$

where T is the transmission, x is the thickness of the lens, and x_0 is the attenuation length. Polycarbonate will lead to lenses that can be constructed easily and inexpensively, but a thick polycarbonate lens may have poor transmission. There are other varieties of plastics that have good UV transmission. These will be investigated in the future.

The other material selected for this study was FC5 glass. This glass is found in the Hoya glass catalog. It is also known as N-FK5 in the Schott catalog and S-FSL 5 in

the OHARA catalog. It has an index of refraction of 1.487 and transmissions are shown in Figure 4 [12]. Its lower index of refraction leads to somewhat thicker lenses, but its transmission over the desired wavelengths is better than polycarbonate.

Design

A.

The first design, denoted lens A, (see Figure 8) has the dimensions shown in Table 1. Once a general design was achieved, certain parameters were set to be adjusted. These parameters included: angular resolution, lens thickness, and input aperture. Throughout the process the complexity of lens was kept at a minimum. Although a few multiple lens designs were conceived, none were seriously pursued. This should keep the cost and difficulty of assembly as low as possible.

One key aspect to the modification of the lens is the angular resolution of the design. It is found using the spot size made on the image plane. Angular resolution was calculated using the following formula, where d_{RMS} is the diameter of the RMS spot size and r is the radius of curvature for the image plane

$$R_a = 180 \times \frac{d_{RMS}}{\pi \times r}$$

For lens A the average angular resolution was found to be 0.60 deg. The best angular resolution was 0.49 deg and the worst 0.68 deg.

Another issue in the lens design was the surface area of the image plane. The image plane represents the cathode material of the photo-sensor. This makes it a very critical factor in the design, because the cathode is expected to be the most expensive part of the photo-sensor. The image surface was made spherical in order to accommodate the

radiation from large angles. The formulas used to calculate the surface area of the plane were

$$S = 2\pi r^2 (1 - \cos \theta)$$

$$\theta = \arcsin \frac{d_s}{r}$$

Where r is the radius of curvature and d_s is the semi diameter of the image plane. Lens A has an image surface area of 54591 mm².

An important parameter is the ratio of the aperture to the overall lens diameter. Lens A had a ratio of 0.39. As we increase the aperture to the desired value (~10cm), we expect all dimensions in Table 1 to increase by the same fraction.

Lens A is the first look at what the final lens needs to be. The advantages of lens A are its simplicity and angular resolution. The disadvantages are the large surface area of the image plane, the thickness of the lens, and the small aperture to lens ratio.

B.

Lens B (Figure 9 and Table 2) was designed to improve on the aperture to lens ratio. Its ratio is 0.57 for the diameters and 0.32 for the area. The surface area of the image plane has also been decreased to 17545 mm². The angular resolution has deteriorated to an average 3.4 deg with a worst of 3.7 deg and a best of 3.1 deg. This lens has improved on both the aperture to lens ratio and the surface area of the lens, and the thickness remains relatively close to lens A. The angular resolution has worsened, but remains within the limits.

C.

The next step was to decrease the thickness of the lens in an attempt to create better transmission, and simplicity. Lens C (Figure 10 and Table 3) was designed for this purpose. The distance between the aperture stop and the lens was increased for this design. In lens B this distance was zero, but now 13 mm of space was inserted. The lens thickness was decreased to 26.11 mm without significantly affecting other factors of the lens. The angular resolution improved to an average of 2.2 deg, best of 1.9 deg, and worst of 2.6 deg. The surface area of the image plane increased to 36698 mm². The aperture to lens ratio decreased to 0.50 in terms of diameter. This lens costs more in image plane surface area and aperture to lens ratio, but was successful in decreasing lens thickness and also improving the angular resolution.

D.

After the thickness was reduced, it was discovered that the lens was still too thick for polycarbonate to be effective. FC5 was substituted in its place because it has better transmission at larger thicknesses. The lens that resulted from this replacement was lens D (Figure 11 and Table 4). The aperture to lens ratio using diameters was 0.52. The surface area of the image plane was 53308 mm², and the thickness was 25.52 mm. The angular resolution was an average of 1.75 deg with a best of 1.53 deg and a worst of 2.02 deg. This lens has actually improved on many factors from lens C including angular resolution, aperture to lens ratio, and thickness.

E.

Another design, lens E (Figure 12 and Table 5), was made with FC5 glass. In this design lens B is re-optimized with FC5 glass. The angular resolution is an average of 4.4

deg, with a best of 3.8 deg and a worst of 5.2 deg. The surface area of the image plane is 18182 mm² and the aperture to lens ratio is 0.60. This lens gives a very compact design, with a small image plane. The problem with lens E is that it has poor angular resolution. This could be improved by small adjustments.

F.

The final step was to increase the aperture to 10 cm. This was done by doubling all the dimensions of lens E. The resulting lens F is displayed in Figure 13 and Table 6. The angular resolution was constant at an average of 4.43 with a best of 3.84 and a worst of 5.17. The surface area of the image plane was 72727 mm², and the aperture to lens ratio remained constant at 0.60.

Conclusions

The properties of all the designs are compared in Table 7. Also the transmittance of the lenses at normal incidence are given at various wavelengths in Table 8. Looking at these graphs it can be concluded that the requirements set at the beginning of this project can be met. All the lenses are able to accept light at angles up to +/- 60 deg using a simple single lens with a water-lens-vacuum geometry. Every design has an average angular resolution within the 5 deg range that was set, with only lenses E and F, traveling outside of this range with their worst resolutions due to spherical aberrations at zero deg. Lenses A, B, and C had poor light transmission over the required wavelength region due to absorption by the polycarbonate material used in this study. However, Lenses D, E, and F were able to suitably transmit light at the required wavelengths to fulfill this condition. Finally, the desired aperture diameter of 10 cm was obtained by lens F.

The next challenge is the detection of the photon at the focal surface. The two options were discussed earlier and depicted in Figure 5. The design in which multiple photo-detectors are to be placed on the image surface would put emphasis on the reduction of the image surface area. The hybrid design which uses a high-voltage field to transport the electron from the photo-cathode needs R&D in several areas: creating the needed high vacuum, depositing photo-cathode on the focal surface, constructing and operating the position sensitive electron detector and providing high voltage to the photo-cathode.

Acknowledgments

This study was conducted at Brookhaven National Laboratory in Upton, NY, through the Science Undergraduate Laboratory Internships (SULI) Program. I would like to thank my mentor, Milind Diwan, for his direction, knowledge, and patience during this appointment. I would also like to thank Peter Takacs, for teaching Milind and I how to design lenses, and Mark Dierckxns, for sharing his office and knowledge with me throughout the summer. This work was supported by DOE grant DE-AC02-98CH10886.

References

- [1] P. Antonioli et al., The AQUA-RICH atmospheric neutrino experiment, Nucl. Inst. And Meth. **A 433** 104-120 (1999).
- [2] S. Fukuda et al., The Super-Kamiokande detector, Nucl. Inst. And Meth., **A 501** 418-462 (2003).
- [3] ZEMAX User's Guide, Focus Software, Inc., P.O. Box 18228, Tuscan, AZ 85731-8228, www.focus-software.com. ZEMAX® is a registered trademark of Focus Software, Inc.
- [4] GEANT - Detector Description and Simulation Tool, NIM A 506 (2003), 250-303.
- [5] R. M. Pope, E. S. Fry, "Absorption spectrum (380-700 nm) of pure water. II. Integrating cavity measurements," *Appl. Opt.*, **36**, 8710-8723, (1997).
- [6] M. Diwan et al., Very long baseline neutrino oscillation experiments for precise measurements of mixing parameters and CP violating effects, Phys. Rev. **D 68**, 012002 (2003). <http://nwg.phy.bnl.gov>
- [7] M. Shiozawa, et al., Search for Proton Decay via $P \rightarrow e^+ \pi^0$ in a Large Water Cerenkov Detector, Phys. Rev. Lett. **81**:3319-3323, (1998).
- [8] K. Eguchi et al. (KamLand Collaboration), Physics Review Letters **90**, 021802 (2003).
- [9] [PDG] Particle Data Group, Review of Particle Physics, Euro. Phys. Jour. **Vol 15**, no. 1-4, 2000.
- [10] John H. Moore, Christopher C. Davis, Michael A. Coplan, Building Scientific Apparatus, pages 119-220, Addison Wesley Publishing Inc., 1989 (second edition).
- [11] M. J. Weber, *Handbook of Optical Materials*. Boca Raton, FL: CRC Press, 2003, pg. 297.
- [12] Optical Glass Master Datasheet, HOYA CORPORATION USA Optics Division, www.hoyaoptics.com.

Figures and Tables

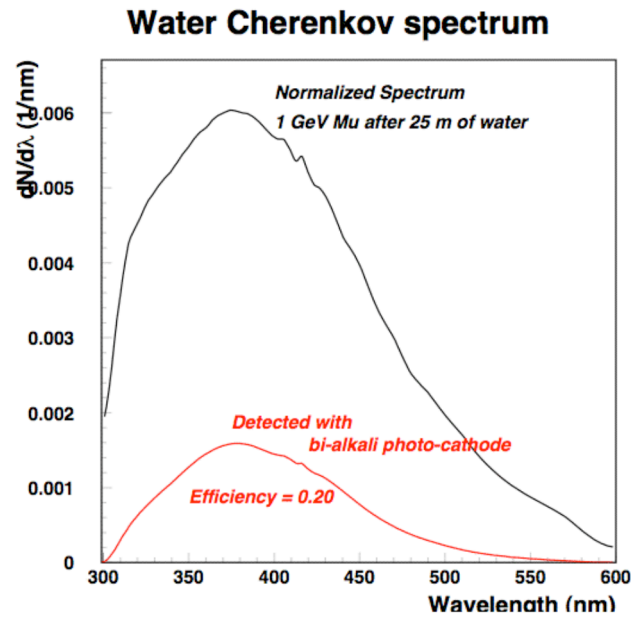


Figure 1 Spectrum of Cherenkov light in pure water calculated for a 1 GeV/c muon at the center of a tank of 50 m diameter. The spectrum includes the effects of absorption as the light travels to the inner surface of the tank. The bottom curve shows the spectrum after including the quantum efficiency of a typical bi-alkali photo cathode.

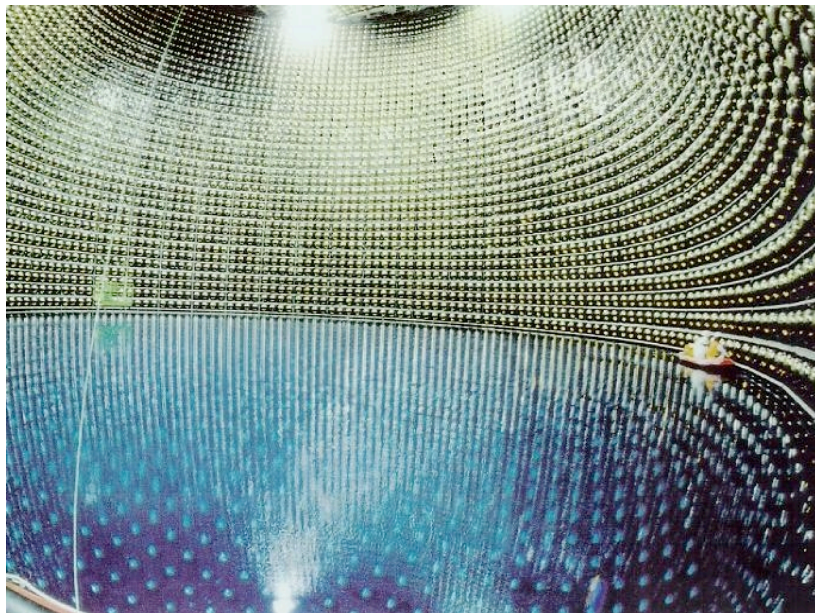


Figure 2 Super Kamiokande detector filled about half-way with water

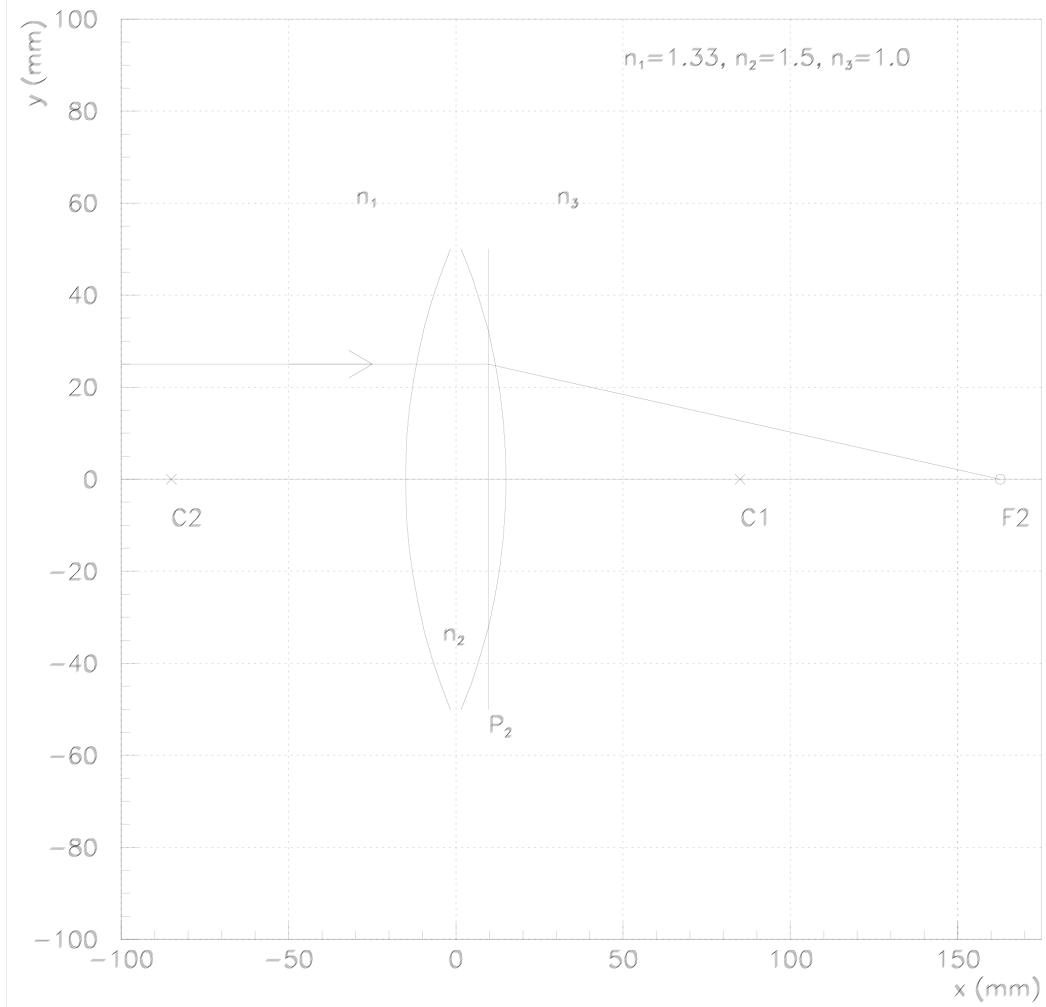


Figure 3 Geometry of a simple thick lens with water on the left side and vacuum on the right hand side.

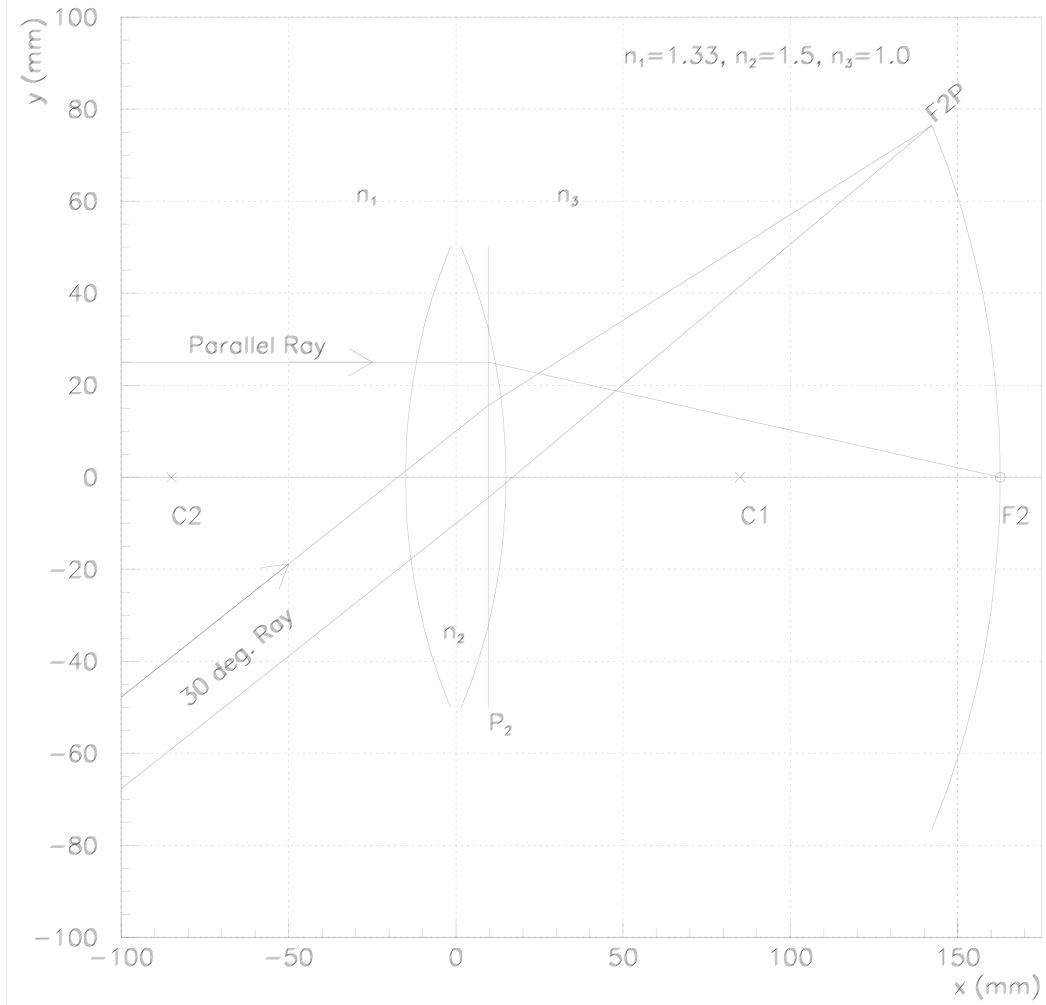


Figure 4 Lens geometry for rays incident at high angles.

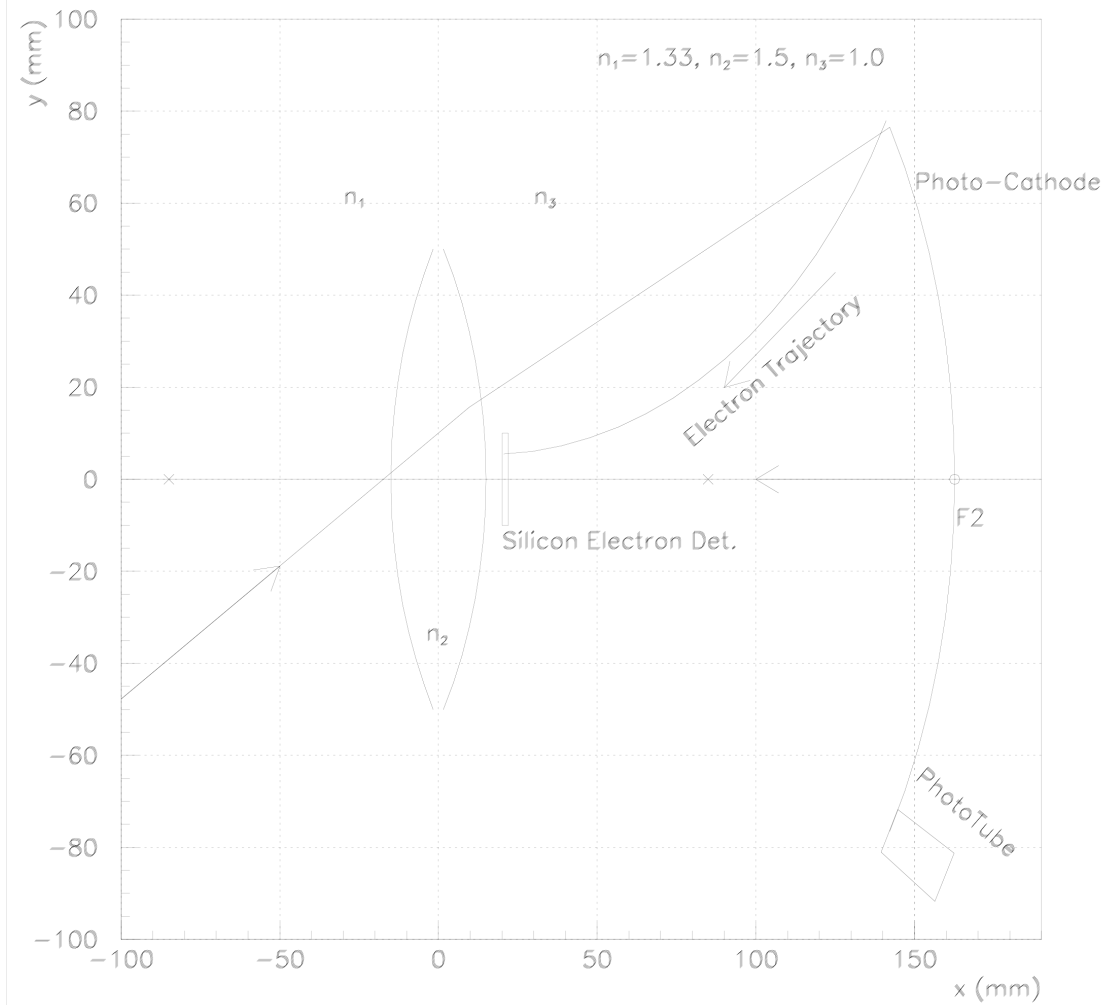
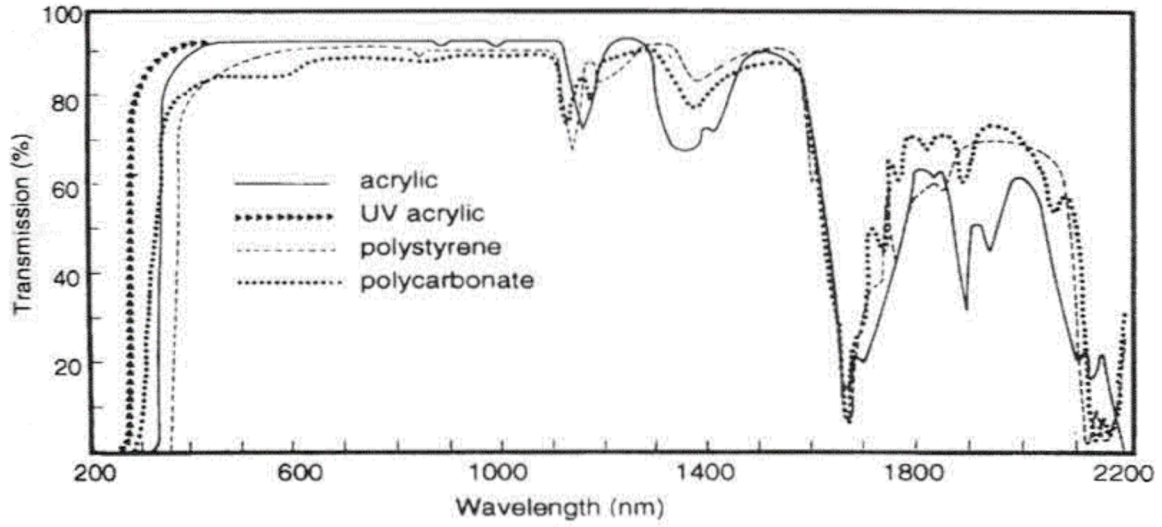


Figure 5 Two possible geometries for placing the photon detectors to construct a direction sensitive photo-sensor.



Transmission spectra of optical plastics. sample thickness: 3.2 mm.

Figure 6 Transmittance of polycarbonate and other materials at a thickness of 3.2 mm [11].

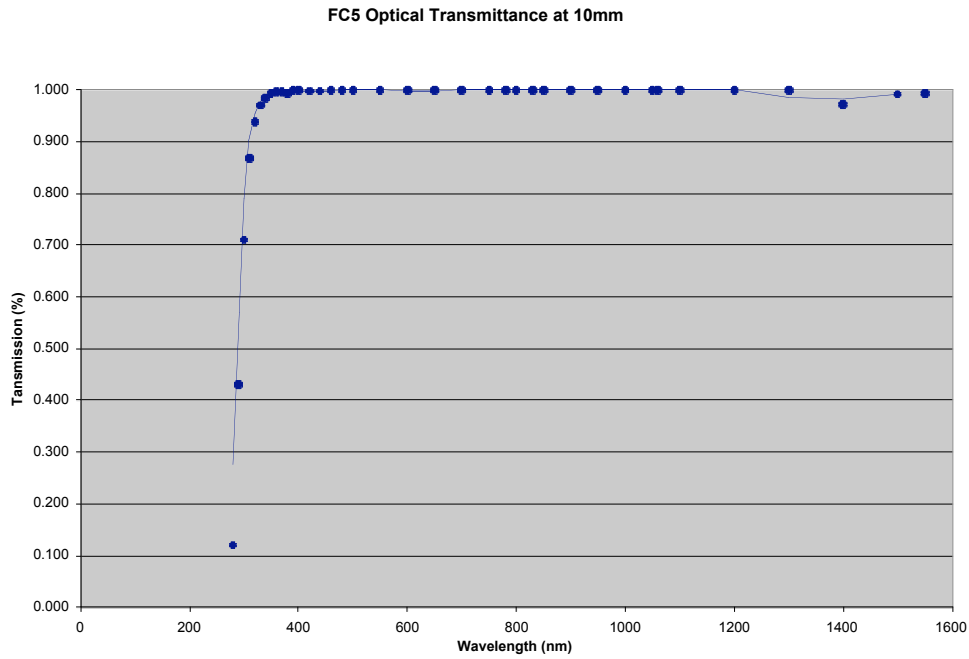


Figure 7 Transmittance of FC5 at 10mm [12].

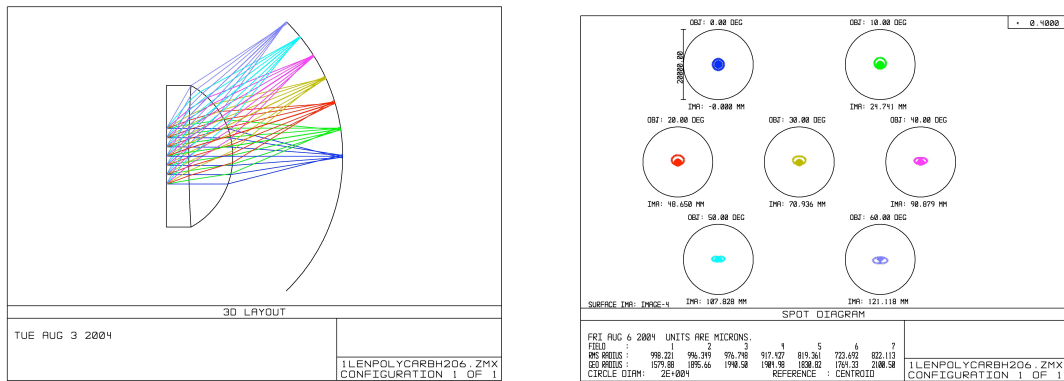


Figure 8 On the left is a ray diagram of lens A. Right side of figure shows the spot diagrams for rays from different angles.

LENS A				
Surface	Composition	Radius (mm)	Thickness (mm)	Semi-diameter (mm)
Object	Water	Infinity	Infinity	Infinity
Stop	Water	Infinity	20.46	25.00
Lens Front	Polycarbonate	1036.00	40.01	63.85
Lens Back	Vacuum	-72.60	100.02	63.84
Image Plane	-	-169.31	-	121.42

Table 1 Table showing dimensions of lens A.

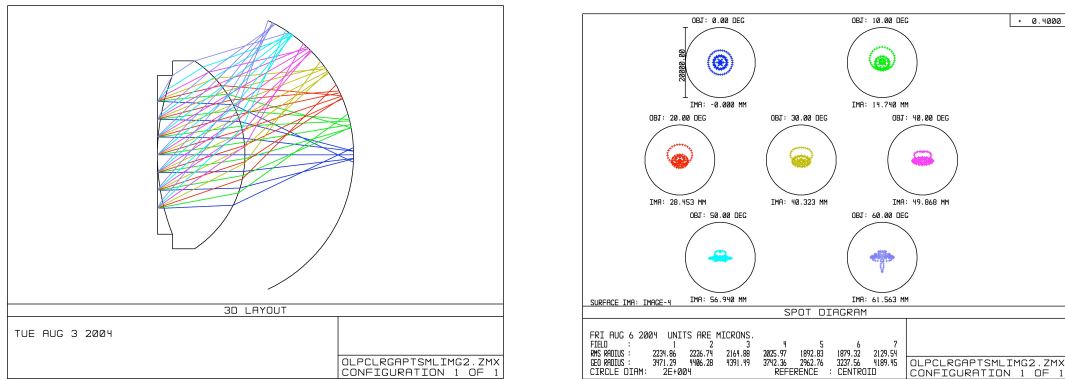


Figure 9 Diagram of lens B.

Lens B				
Surface	Composition	Radius (mm)	Thickness(mm)	Semi-diameter (mm)
Object	Water	Infinity	Infinity	Infinity
Stop	Water	Infinity	0.00	25.00
Lens Front	Polycarbonate	101.65	41.16	37.24
Lens Back	Vacuum	-52.71	51.08	44.05
Image Plane	Vacuum	-69.39	-	62.97

Table 2 Table showing dimensions of lens B.

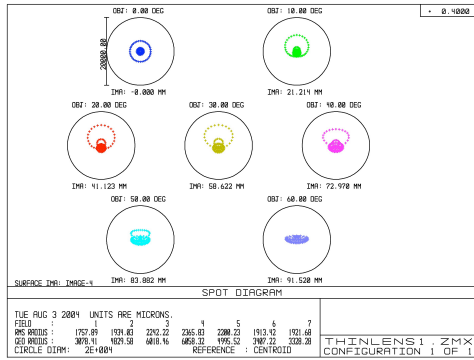
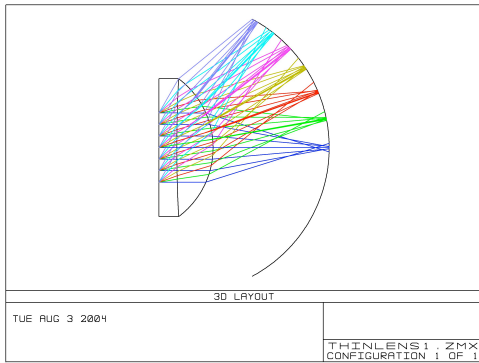


Figure 10 Diagram of lens C.

LENS C				
Surface	Composition	Radius (mm)	Thickness (mm)	Semi-diameter (mm)
Object	Water	Infinity	Infinity	Infinity
Stop	Water	Infinity	13.00	25.00
Lens Front	Polycarbonate	968.80	26.11	49.73
Lens Back	Vacuum	-62.20	83.74	49.73
Image Plane	Vacuum	-105.22	-	92.74

Table 3 Table showing dimensions of Lens C.

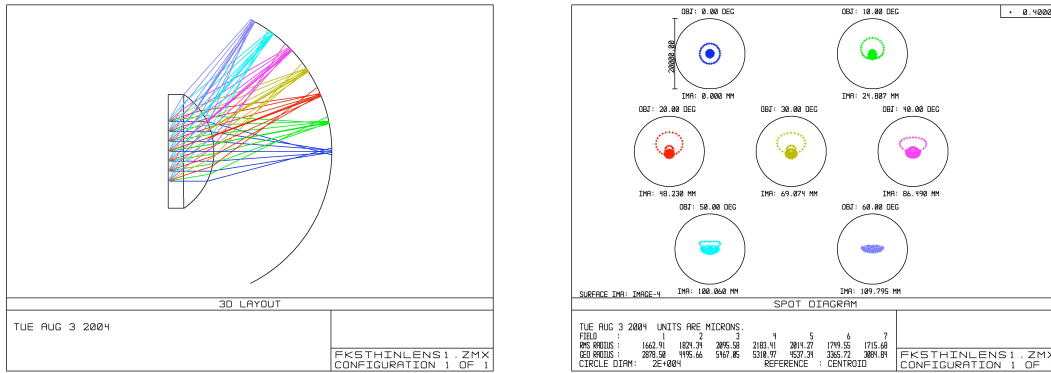


Figure 11 Diagram of lens D.

LENS D				
Surface	Composition	Radius (mm)	Thickness (mm)	Semi-diameter (mm)
Object	Water	Infinity	Infinity	Infinity
Stop	Water	Infinity	13.00	25.00
Lens Front	FC5	6582.03	25.52	47.82
Lens Back	Vacuum	-57.78	99.49	47.82
Image Plane	Vacuum	-123.83	-	110.79

Table 4 Table showing dimensions of lens D.

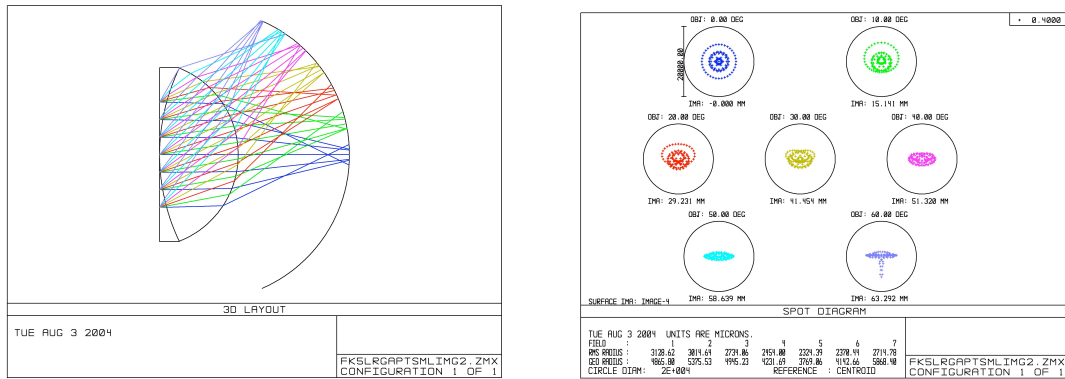


Figure 12 Diagram of lens E.

Lens E				
Surface	Composition	Radius (mm)	Thickness (mm)	Semi-diameter (mm)
Object	Water	Infinity	Infinity	Infinity
Stop	Water	Infinity	0.00	25.00
Lens Front	FC5	95.29	37.51	41.35
Lens Back	Vacuum	-44.17	53.12	41.20
Image Plane	-	-69.30	-	63.59

Table 5 Table showing dimensions of lens E.

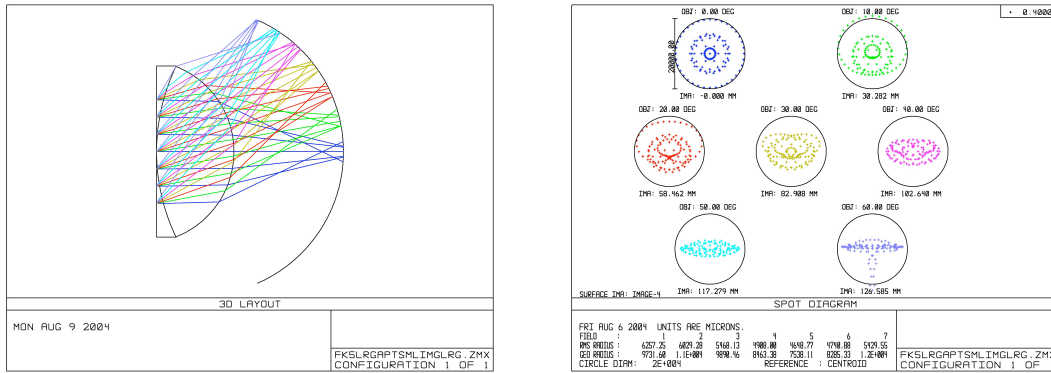


Figure 13 Diagram of lens F.

Lens F				
Surface	Composition	Radius (mm)	Thickness(mm)	Semi-diameter(mm)
Object	Water	Infinity	Infinity	Infinity
Stop	Water	Infinity	0.00	50.00
Lens Front	FC5	190.58	75.02	82.69
Lens Back	Vacuum	-88.33	106.24	82.40
Image Plane	Vacuum	-138.60	-	127.18

Table 6 Table showing dimensions of lens F.

Lens	A	B	C	D	E	F
Avg. Angular Resolution (deg)	0.605	3.433	2.230	1.750	4.427	4.427
Best Angular Resolution (deg)	0.490	3.103	1.915	1.538	3.844	3.844
Worst Angular Resolution (deg)	0.676	3.691	2.577	2.021	5.173	5.173
Surface Area (mm²)	54591	17545	36698	53308	18182	72727
Aperture to Lens Ratio	0.392	0.567	0.503	0.523	0.605	.605
Aperture to Lens Ratio (Area)	0.153	0.322	0.253	0.273	0.366	0.366

Table 7 Table displaying various properties of the different lenses.

		Wavelength (nm)								
		600	550	500	480	460	440	420	400	390
Lens	A	0.517	0.503	0.503	0.503	0.503	0.491	0.450	0.445	0.422
	B	0.479	0.464	0.464	0.464	0.464	0.452	0.410	0.406	0.382
	C	0.650	0.638	0.638	0.638	0.638	0.628	0.594	0.590	0.569
	D	0.996	0.996	0.996	0.996	0.993	0.989	0.989	0.993	0.993
	E	0.997	0.997	0.997	0.997	0.995	0.992	0.992	0.995	0.995
	F	0.993	0.993	0.993	0.993	0.985	0.978	0.978	0.985	0.985
		Wavelength (nm)								
		380	370	360	350	340	330	320	310	300
Lens	A	0.401	0.385	0.355	0.328	0.124	0.069	0.036	0.006	0.000
	B	0.361	0.345	0.315	0.289	0.098	0.050	0.024	0.003	0.000
	C	0.551	0.537	0.509	0.483	0.257	0.174	0.114	0.035	0.002
	D	0.974	0.985	0.981	0.970	0.941	0.892	0.783	0.588	0.277
	E	0.982	0.990	0.987	0.980	0.960	0.926	0.848	0.699	0.420
	F	0.949	0.970	0.963	0.942	0.886	0.796	0.614	0.346	0.077

Table 8 Table showing transmittance of lenses at their individual thicknesses.

